

Effect of the MgO substitution for CuO on the properties of $\text{CaCu}_3\text{Ti}_4\text{O}_{12}$ ceramics

Yi Hu ^{*}, Tian-Syuan Jeng, Jiun-Shing Liu

Department of Materials Engineering, Tatung University, Taipei, Taiwan, ROC

Received 1 November 2011; received in revised form 21 December 2011; accepted 21 December 2011

Available online 31 December 2011

Abstract

In this work, the effect of MgO substitution for CuO on the dielectric properties of $\text{CaCu}_3\text{Ti}_4\text{O}_{12}$ (CCTO) was studied. Ceramic samples of $\text{CaCu}_{3-x}\text{Mg}_x\text{Ti}_4\text{O}_{12}$ were prepared by a two-step solid-state reaction. The samples were sintered at 600 °C for 2 h and then heated to the final sintering temperature of 1100 °C for 8 h. The lattice parameter of CCTO decreases with Mg substitution from X-ray diffraction (XRD) analysis, since the ionic radius of Mg^{2+} is smaller than that of Cu^{2+} . Mg substitution in CCTO causes apparent change in microstructure with much smaller grains due to the grain growth inhibition. The maximum of the dielectric constant can reach to 7.8×10^5 at $f = 100$ Hz for Mg substitution with $x = 0.6$. The sample with Mg substitution ($x > 0.2$) yields an apparent semicircle in the impedance spectra. The correlation between the microstructure and dielectric properties suggests the presence of a thin barrier layer forming at the grain boundary.

© 2012 Elsevier Ltd and Techna Group S.r.l. All rights reserved.

Keywords: C. Impedance; Giant dielectric; Ceramics; Substitution

1. Introduction

Recently, the perovskite material $\text{CaCu}_3\text{Ti}_4\text{O}_{12}$ (CCTO) has attracted much attention due to its so-called “giant dielectric effect” [1–5]. The CCTO ceramics display unusual dielectric properties with a high permittivity up to 10^5 over wide frequency (10^2 – 10^6 Hz). The high permittivity of CCTO has been interpreted as from the effect of internal barrier layer capacitor (IBLC) [4]. Polarization effects at insulating grain boundaries between semiconducting grains or other internal barriers are responsible for the colossal dielectric constant. The interfacial polarization termed Maxwell–Wager relaxation between the electrodes and the sample surfaces was also proposed to explain the giant dielectric effect [6].

Many efforts have been made to improve their electric properties by tailoring the compositions of CCTO. It was reported that the dielectric loss at low frequencies ($f < 10^4$ Hz) could be reduced by adding CaTiO_3 [7,8] and ZrO_2 [9] to increase the resistance of the barrier layers. It has been also reported that small amount substitutions of transition ions, such

as Mn, Cr, and V in the octahedral Ti site and La in the Ca site, can yield changes of the magnetic and dielectric properties [10,11]. Other ions doping such as Co, Ni, and Fe has been shown to increase the dielectric constant of CCTO dramatically by the substitution for Cu [12]. Doping or substitution method opens an effective way to tailor the electric performance as mentioned above.

The structure of CCTO as known is the body-centered cubic perovskite-related structure. The Ca^{2+} ion is dodecahedrally coordinated with oxygen ions, Cu^{2+} is in a square-planar coordination and Ti^{4+} coordinates six oxygen ions in cell axis [1–3]. The copper ion in this structure has been discussed in a Jahn–Teller context, which strongly promotes stoichiometry of CCTO as suggested [13]. This may be ascribed to the complex valence of copper ions. Recently, it was reported that No second phase is detected in CCTO with small amount of Mg doping [14]. The valence of copper ion changed with Mg doping in CCTO and causes an enhancement in dielectric property as reported. In this literature the solubility of Mg in CCTO is small due to the relative lower sintering temperature (1000 °C). However, the solubility can be elevated by increasing the sintering temperature. In this work, MgO was added to substitute Cu ions in CCTO with higher sintering temperature to investigate role of the Mg in CCTO.

^{*} Corresponding author. Tel.: +886 2 25925252x3411; fax: +886 2 25936897.

E-mail address: huyi@ttu.edu.tw (Y. Hu).

2. Experimental

Ceramic samples of $\text{CaCu}_{3-x}\text{Mg}_x\text{Ti}_4\text{O}_{12}$ ($x = 0, 0.2, 0.4, 0.6, 0.8$ and 1.0) were prepared by a conventional two-step solid-state reaction. The starting materials were high purity 99.9% CaO , CuO , MgO , and TiO_2 . They were weighted according to the stoichiometric ratios and mixed thoroughly by ball milling with ZrO_2 balls for 24 h. The mixture was calcined at 900°C for 6 h in air. Then the calcined powder was pulverized and wet-mixed with 1.5 wt% PVA. The powders were pressed into disks with 19.5 mm in diameter and 1.5 mm of thickness under 100 MPa. The disks were sintered in air from room temperature to the intermediate 600°C for 2 h with $2^\circ\text{C}/\text{min}$. When the intermediate temperature was reached, the samples were then heated to the sintering temperature of 1200°C for 8 h with $5^\circ\text{C}/\text{min}$ and furnace-cooled to room temperature.

The crystallographic structures of the disk samples were examined by X-ray diffraction (XRD, MAC Science M18XHF) with $\text{CuK}\alpha$ irradiation. The density of the sintered samples was measured with Archimedes' method. The microstructures of the sample's surfaces were examined by scanning electron microscope (JEOL-5600 SEM). The capacitance (C_p) and the dissipation factor ($\tan \delta$) of the sample were measured with a parallel-plate capacitor coupled to a precision LCR meter (HP 4284A) at an ac voltage of 1 V in the frequency range from 20 Hz to 1 MHz. The ϵ' value was obtained from capacitance (C_p) and the dimension of the sample (the thickness and the area of the electrode). The complex impedance was obtained by the equation $Z^* = 1/(i\omega C^*)$, where $C^* = C_p(1 - i\tan \delta)$ and $\omega = 2\pi f$.

3. Results and discussion

The X-ray diffraction (XRD) patterns of the samples are shown in Fig. 1. The sample without MgO substitution shows a predominant CCTO phase of cubic perovskite structure and a small amount of second phase, rutile TiO_2 , as in Fig. 1(a) with $x = 0$. The second phase (TiO_2) is not observed for the sample with MgO substitution for $x > 0.2$. Nevertheless, it was found that the intensity of (4 2 2) plane reflection decreased apparently relative to other plane reflections with the increase of MgO content. The refraction intensity of (4 2 2) plane to that of (2 2 0) plane used to illustrate the effect of MgO substitution is shown in Fig. 2. This may be attributed to the increase in surface energy by the MgO substitution for CuO . The ionic radius of Mg^{2+} (0.49 \AA) with 4 coordination is smaller than that of Cu^{2+} (0.62 \AA) and the bond strength of Mg-O (1.09) is larger than that of Cu-O (1.01) [15]. (The bond strength is defined as the ratio of valence over internuclear distance.) This surface energy of (4 2 2) plane based on the bonding strength became lower relative to other planes indicates that the sites occupied by Mg ions are less on the (4 2 2) plane. Therefore, the most possible sites for the Mg ions occupying is the face center positions of the cubic perovskite structure such as $0, 0, 0$, and 0 .

In addition, the lattice parameter of CCTO would decrease with MgO substitution for CuO due to the fact that Mg^{2+} ($r \sim 0.49 \text{ \AA}$) has smaller ionic radius than Cu^{2+} ($r \sim 0.62 \text{ \AA}$).

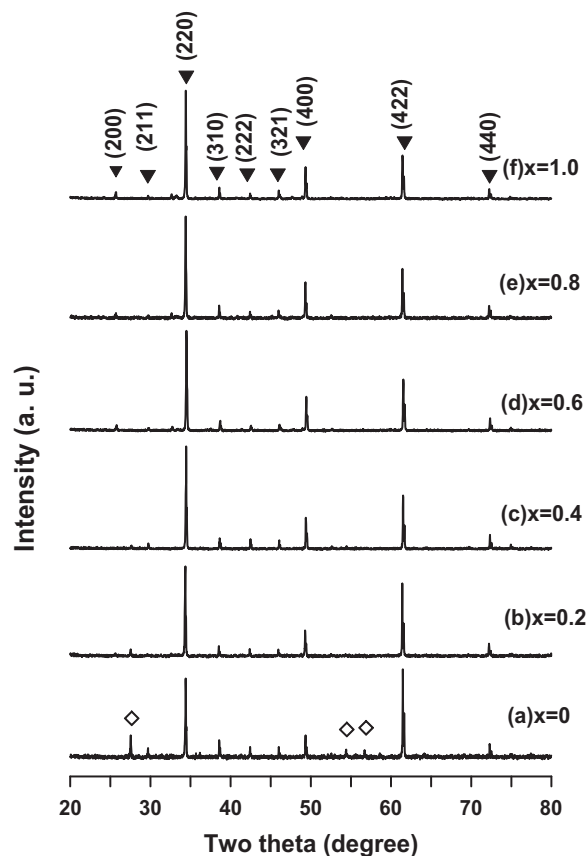


Fig. 1. X-ray diffraction patterns of samples sintered at 1200°C as a function of x value for $\text{CaCu}_{3-x}\text{Mg}_x\text{Ti}_4\text{O}_{12}$ (◆, CCTO phase; ◇, TiO_2 rutile).

Fig. 3 shows the shift of the (4 2 2) plane diffraction peaks of the samples with different Mg content. The (4 2 2) diffraction peak shifting to larger angle is ascribed to the decrease in the lattice constant by MgO substitution. The shift of the diffraction peak and dissolution of second phase from the result of XRD analysis would thus confirm that Mg can substitute into the lattice of CCTO crystal lattice.

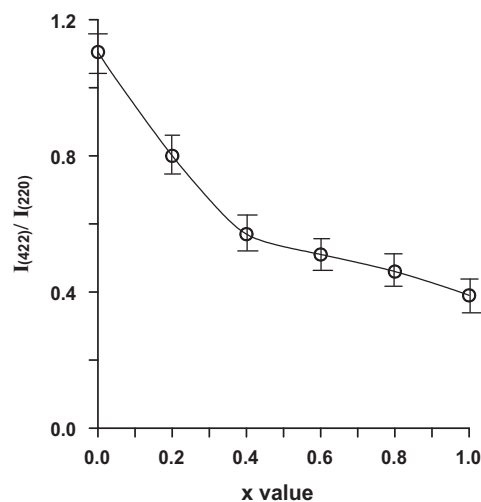


Fig. 2. The relative intensity of the XRD peaks of (4 2 2) plane to (2 2 0) plane of CCTO phase as a function of x value for $\text{CaCu}_{3-x}\text{Mg}_x\text{Ti}_4\text{O}_{12}$.

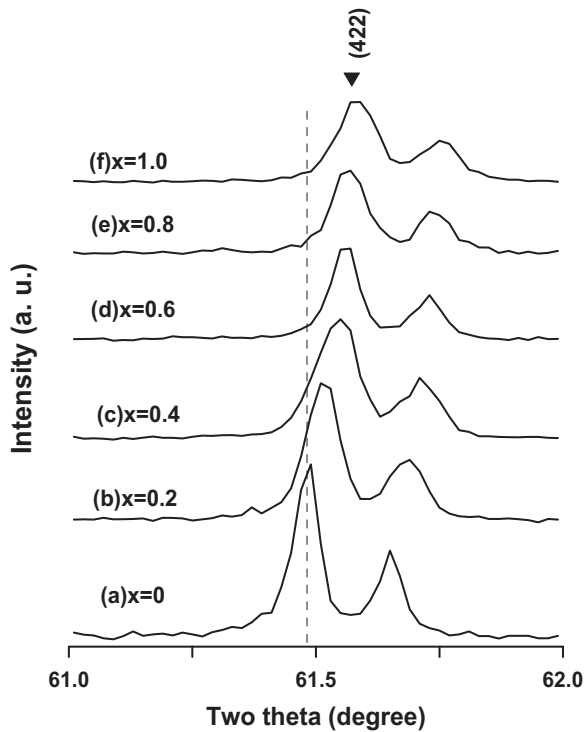


Fig. 3. Expanded XRD patterns of the (4 2 2) reflection of CCTO phase for the samples as a function of x value indicating the shift of the peaks.

Fig. 4 gives SEM images of the surface morphologies of the sample sintered at 1200 °C for 8 h. In pure CCTO ceramics, the microstructure shows abnormally grains with very small grains segregating at the grain boundaries as in Fig. 4(a). The small grains at the grain boundaries are pointed with arrows. Similar result in microstructure of CCTO has also been reported in the literature [16]. The mechanism for the grain growth of CCTO based on the CuO liquid sintering phase has been reported by Leret et al. [17]. The Cu-rich phases formed from the reoxidization of the liquid Cu_2O , which is initially reduced from CuO at temperatures higher than 1000 °C. These small grains of Cu-rich phases segregated at the grooved grain boundaries and lead the grains had the non-stoichiometric composition of the CCTO. On the other hand, it was found that the grain size of the sample decreased apparently and the segregated small grains disappeared when the Mg content increased ($x > 0.2$). The shape of the some grains changes from large abnormal grains to small equiaxial grains. This is attributed to that the grain growth was inhibited by raising the melting temperature with the formation of CuO–MgO solid solution. Such a solid solution with higher melting temperature would cause lower mobility of the ions. The inhibition of grain growth may also be ascribed to the distortion of lattice with MgO substitution for CuO.

Figs. 5 and 6 show the results of broadband dielectric constant and tangent loss for the samples versus frequency, respectively. Colossal values of $\epsilon' \sim 1.5 \times 10^4$ are obtained for the sample without MgO substitution ($x = 0$). Since the dielectric constant of TiO_2 ($\epsilon \sim 85$) is much lower comparing to CCTO phase, the effect of the appearance of TiO_2 on the dielectric constant may be

neglected based on the series connection of capacitance of each phase. It has also been reported that the presence of TiO_2 minor phase in CCTO ceramics showed no influence on the dielectric permittivity [18]. On the other hand, the formation of TiO_2 would result in the formation of intergranular Cu-rich phase and significantly affected the relative dielectric permittivity and dielectric loss [19]. The CuO-rich intergranular phase can be regarded as a predominant reason for the deterioration of dielectric properties.

The dielectric constant of the samples largely increased with MgO substitution in the frequency range ($f < 10^4$ Hz) as in Fig. 5. The maximum of the dielectric constant can reach to 7.8×10^5 at $f = 100$ Hz with Mg substitution of $x = 0.6$. Similar high dielectric constants higher than 10^5 were also observed in CCTO ceramics doped with Co^{2+} , Ni^{2+} , and Fe^{2+} even at low frequency by Chiodelli et al. [20]. Some other doping species such as Mn^{2+} , Sr^{2+} , Fe^{3+} , Zr^{4+} and La^{3+} would cause decrease in the dielectric constant and lowering in dielectric loss [9,11,21–23]. However, the effects of high substitution on dielectric properties for CCTO ceramics have not been widely investigated. The dielectric constant is predominantly affected by the grain size and microstructure and varied largely from 10^3 to 10^5 [24]. It was thus postulated that the variation in dielectric constant of CCTO ceramics by doping or substitution is ascribed to the change in grain size and microstructure as observed in Fig. 4.

CCTO was dramatically increased by such doping. The correlations between the microstructures and dielectric properties of CCTO polycrystalline ceramics have been reported that the decrease in the ϵ_r values in the relatively low frequency region is proportional to the decrease in the size and number of abnormally grown grains [25]. However, the dielectric constant of the samples increased largely as the grain size decreased in this study. This could not be ascribed to the increase of ionic polarization by MgO substitution, since the polarization ability of Mg^{2+} ($\alpha \sim 0.094$) is lower than that of Cu^{2+} ($\alpha \sim 0.437$) [26]. On the other hand, these materials may present a so-called giant dielectric permittivity, which generally associated with an internal barrier layer capacitor (IBLC) effect [20,27,28]. According to this model, CCTO ceramics are constituted of semi-conducting grains (pure CCTO phase), and insulating grain boundary layers. The increase in the dielectric constant with MgO substitution may be attributed the formation of the insulating grain boundary layers with Mg-rich phase.

The well-known relaxation steps (Debye-like relaxation) was not observed in the frequency range $f < 1$ MHz for the sample with $x = 0$ and $x = 0.2$. However, the relaxation steps with a decrease in ϵ' (Fig. 5) at the frequency, where $\tan \delta$ displays a relaxation peak as in Fig. 6, were observed for the sample with Mg substitution of $x = 0.6$ to $x = 1.0$. It was found that the frequency for the relaxation was at about 10^4 Hz. Such a relaxation is generally suggested as the Maxwell–Wagner (MW) type relaxation, which can be illustrated with an equivalent circuit consisting of the bulk contribution, connected in series to a parallel RC circuit [4]. The highly resistive thin layers, which generate this RC circuit, could be from the grain boundaries in this study.

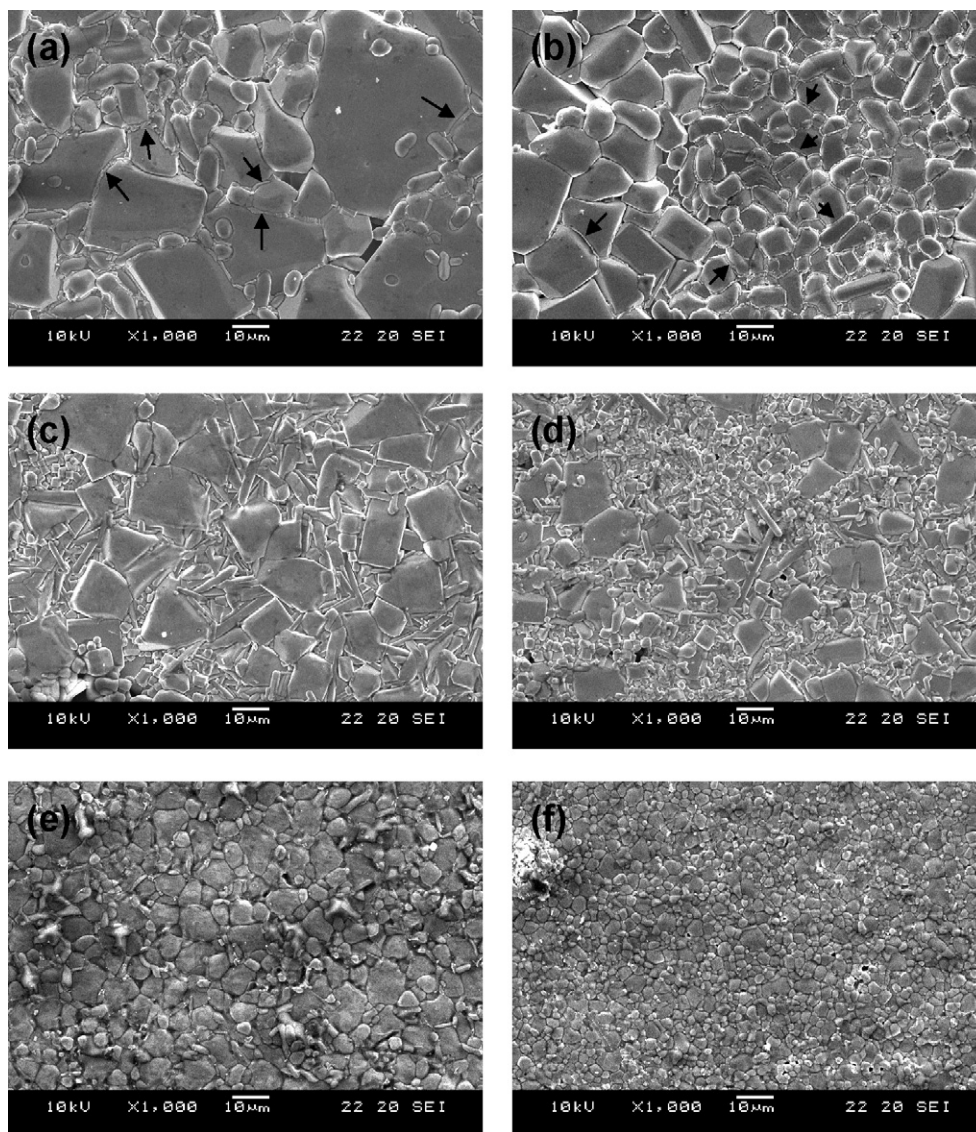


Fig. 4. SEM photographs of the surface of the samples with (a) $x = 0$, (b) $x = 0.2$, (c) $x = 0.4$, (d) $x = 0.8$, and (e) $x = 1.0$ for $\text{CaCu}_{3-x}\text{Mg}_x\text{Ti}_4\text{O}_{12}$.

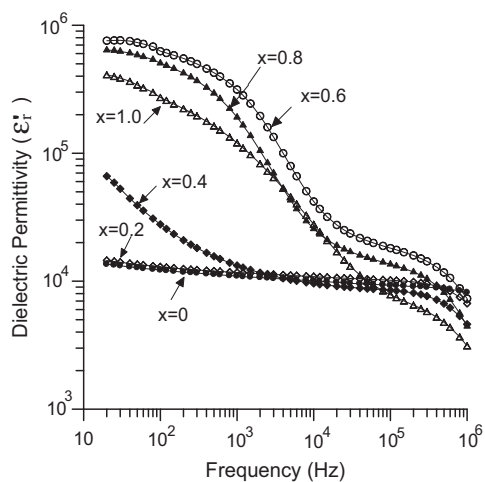


Fig. 5. Frequency dependence of the dielectric constant (ϵ') as a function of x value for $\text{CaCu}_{3-x}\text{Mg}_x\text{Ti}_4\text{O}_{12}$.

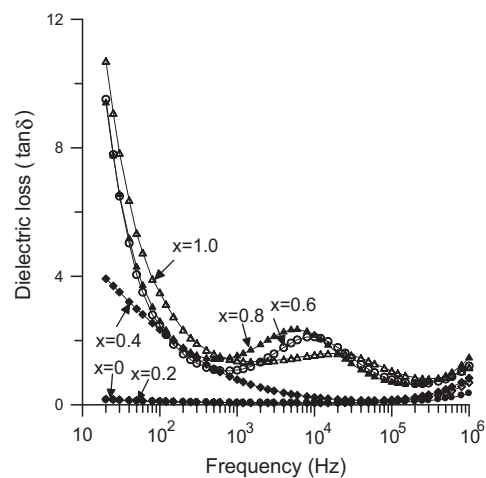


Fig. 6. Frequency dependence of the dielectric loss ($\tan \delta$) as a function of x value for $\text{CaCu}_{3-x}\text{Mg}_x\text{Ti}_4\text{O}_{12}$.

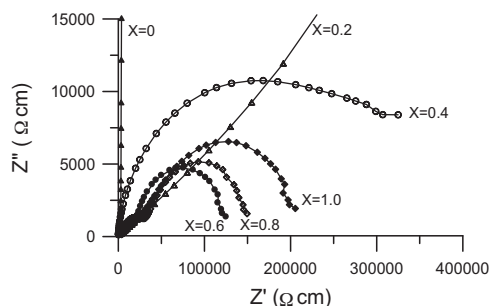


Fig. 7. Complex impedance plot Z'' versus Z' at room temperature as a function of x value.

Fig. 7 shows the impedance spectra of the samples as a function of frequency. The resistivity of the sample without MgO substitution ($x = 0$) is about $9.5 \times 10^5 \Omega \text{ cm}$ at $f = 20 \text{ Hz}$. The segregated small grains with Cu-rich phases formed at the grain boundary do not give the half-circles of impedance in the range of frequency for $x = 0$ and $x = 0.2$. Since the samples did not present a complete semicircle, they could not be considered for equivalent circuit modeling with ideal resistors and capacitors in the RC equivalent circuit. On the other hand, as shown in Fig. 7, the impedance spectra of the samples with Mg substitution ($x > 0.2$) yield apparent semicircles, which is usually corresponding to the electrical response of grain boundaries. The semicircle diameter gives the electrical resistivity of the sample and the maximum value corresponds to the relaxation frequency. The semicircle diameter of the samples increased as the Mg content increased for the x from 0.6 to 1.0. This indicates that the resistance of the boundary layer increased as the Mg content increased for the x from 0.6 to 1.0.

The arcs or semicircles response in the impedance spectra can be revealed by the conductivity of the grain and grain boundary. Usually, the arcs for the CCTO ceramics are thought as consisting of semiconducting grains and boundary layers regions with much larger resistance. The semiconductivity may possibly arise from the non-stoichiometric composition of the CCTO by the segregation of copper. The segregation of copper would not cause apparent difference in conductivity between grain and grain boundary. Therefore, no apparent arc in the impedance spectra was observed for the sample without Mg substitution. On the other hand, the larger resistance of boundary layer is explained by the formation of Mg-rich phases at grain boundaries as insulating barriers in the ceramic.

This study revealed that the Mg substitution for Cu can control the grain size of CCTO ceramics, which is an important factor to adjust the electric properties of internal barrier layer capacitors. The finding of huge dielectric constant in Mg substituted CCTO provided a feasible application in the technology of high energy density capacitors. However, in the current study, Mg substitution for Cu yielded a higher dielectric loss ($\tan \delta$). A high loss greatly blocks its use in electronic industry. Further work on lowering the loss while remaining the high dielectric constant becomes desirable.

4. Conclusions

Ceramics with small amount of MgO substitution for CuO with nominal composition of $\text{CaCu}_{3-x}\text{Mg}_x\text{Ti}_4\text{O}_{12}$ ($x = 0-1.0$) were obtained by two-step solid state reaction method. The results show that CCTO ceramics with MgO substitution exhibit Cubic perovskite single phase and the abnormal growth grain gradually disappears and grains become obviously uniform and fine by inhibiting the grain growth. The change in lattice constant confirms that Mg substitute into the lattice of CCTO from the XRD analysis. The impedance spectra of the sample with Mg substitution ($x > 0.2$) yield an apparent semicircle due to the electrical response of grain boundaries. Such results are attributed to the presence of insulating grain-boundary barrier layers.

Acknowledgment

Financial support of this research by National Science Council, Taiwan, ROC, under the grant NSC 98-2221-E-036-012 is gratefully acknowledged.

References

- [1] M.A. Subramanian, D. Li, N. Duan, B. Reisner, A.W. Sleight, High dielectric constant in $\text{ACu}_3\text{Ti}_4\text{O}_{12}$ and $\text{ACu}_3\text{Ti}_3\text{FeO}_{12}$ phases, *J. Solid State Chem.* 151 (2000) 323–325.
- [2] A.P. Ramirez, M.A. Subramanian, M. Gradel, G. Blumberg, D. Li, T. Vogt, S.M. Shapiro, Giant dielectric constant response in a copper–titanate, *Solid State Commun.* 115 (2000) 217–220.
- [3] C.C. Homes, T. Vogt, S.M. Shapiro, S. Wakimoto, A. Ramirez, Optical response of high-dielectric-constant perovskite-related oxide, *Science* 293 (2001) 673–676.
- [4] D.C. Sinclair, T.B. Adams, F.D. Morrison, A.R. West, $\text{CaCu}_3\text{Ti}_4\text{O}_{12}$: one-step internal barrier layer capacitor, *Appl. Phys. Lett.* 80 (2002) 2153–2155.
- [5] M.H. Cohen, J.B. Neaton, L. He, d. Vanderbilt, Extrinsic models for the dielectric response of $\text{CaCu}_3\text{Ti}_4\text{O}_{12}$, *J. Appl. Phys.* 94 (2003) 3299–3306.
- [6] P. Lunkenheimer, V. Bobnar, A.V. Pronin, A.I. Ritus, A.A. Volkov, A. Loidl, Origin of apparent colossal dielectric constants, *Phys. Rev. B* 66 (2002), 052105 (1–4).
- [7] W. Kobayashi, I. Terasaki, $\text{CaCu}_3\text{Ti}_4\text{O}_{12}/\text{CaTiO}_3$ composite dielectrics: Ba/Pb-free dielectric ceramics with high dielectric constants, *Appl. Phys. Lett.* 87 (2005) 032902–32904.
- [8] Y.Y. Yan, L. Jin, L.X. Feng, G.H. Cao, Decrease of dielectric loss in giant dielectric constant $\text{CaCu}_3\text{Ti}_4\text{O}_{12}$ ceramics by adding CaTiO_3 , *Mater. Sci. Eng. B* 130 (2006) 146–150.
- [9] E.A. Patterson, S. Kwon, C.C. Huang, D.P. Cann, Effects of ZrO_2 additions on the dielectric properties of $\text{CaCu}_3\text{Ti}_4\text{O}_{12}$, *Appl. Phys. Lett.* 87 (2005) 182911–182913.
- [10] M.C. Mozatti, C.B. Azzoni, D. Capsoni, M. Bini, V. Massarotti, Electron paramagnetic resonance investigation of polycrystalline $\text{CaCu}_3\text{Ti}_4\text{O}_{12}$, *J. Phys: Condens. Matter* 15 (2003) 7365–7374.
- [11] L. Feng, X. Tang, Y. Yan, X. Chen, Z. Jiao, G. Cao, Decrease of dielectric loss in $\text{CaCu}_3\text{Ti}_4\text{O}_{12}$ ceramics by La doping, *Phys. Status Solidi A* 203 (2006) R22–R24.
- [12] J. Li, M.A. Subramanian, H.D. Rosenfeld, C.Y. Jones, B.H. Toby, A.W. Sleight, Clues to the giant dielectric constant of $\text{CaCu}_3\text{Ti}_4\text{O}_{12}$ in the defect structure $\text{SrCu}_3\text{Ti}_4\text{O}_{12}$, *Chem. Mater. Commun.* 16 (2004) 5223–5225.
- [13] C. Lacroix, Crystallographic and magnetic structures of materials with threefold orbital degeneracy: application to $\text{CaCu}_3\text{Ti}_4\text{O}_{12}$, *J. Phys. C* 13 (1980) 5125–5136.

- [14] M. Li, Gemei Cai, D.F. Zhang, W.Y. Wang, W.J. Wang, X.L. Chen, Enhanced dielectric responses in Mg-doped $\text{CaCu}_3\text{Ti}_4\text{O}_{12}$, *J. Appl. Phys.* 104 (2008) 074107–74114.
- [15] R.D. Shannon, C.T. Preitt, Effective ionic radii in oxides and fluorides, *Acta Crystallogr. B* 25 (1969) 925–946.
- [16] S.-Y. Lee, D.-k. Yoo, S.-I. Yoo, Microstructures and dielectric properties of Cu-deficient and excess $\text{CaCu}_3\text{Ti}_4\text{O}_{12}$ polycrystalline ceramics, *Electron. Mater. Lett.* 3 (2007) 23–25.
- [17] P. Leret, J.F. Fernandez, J. de Frutos, D. Fern, E.Z. Hevia, Nonlinear I–V electrical behaviour of doped $\text{CaCu}_3\text{Ti}_4\text{O}_{12}$ ceramics, *J. Eur. Ceram. Soc.* 27 (2007) 3901–3905.
- [18] B. Barbier, C. Combettes, S. Guillemet-Fritsch, T. Chartier, F. Rossignol, A. Rumeaud, T. Lebey, E. Dutarde, $\text{CaCu}_3\text{Ti}_4\text{O}_{12}$ ceramics from co-precipitation method: dielectric properties of pellets and thick films, *J. Eur. Ceram. Soc.* 29 (2009) 731–735.
- [19] G. Cao, L. Feng, C. Wang, Grain-boundary and subgrain-boundary effects on the dielectric properties of $\text{CaCu}_3\text{Ti}_4\text{O}_{12}$ ceramics, *J. Phys. D: Appl. Phys.* 40 (2007) 2899–2905.
- [20] G. Chiodelli, V. Massarotti, D. Capsoni, M. Bini, C.B. Azzoni, M.C. Mozzati, Electric and dielectric properties of pure and doped $\text{CaCu}_3\text{Ti}_4\text{O}_{12}$ perovskite materials, *Solid State Commun.* 132 (2004) 241–246.
- [21] S. Krohns, J. Lu, P. Lunkenheimer, V. Brizé, C. Autret-Lambert, M. Gervais, F. Gervais, F. Bourée, F. Porcher, A. Loidl, Correlations of structural, magnetic, and dielectric properties of undoped and doped $\text{CaCu}_3\text{Ti}_4\text{O}_{12}$, *Eur. Phys. J. B* 72 (2009) 173–182.
- [22] R. Schmidt, D.C. Sinclair, Anomalous increase of dielectric permittivity in Sr-doped CCTO ceramics $\text{Ca}_{1-x}\text{Sr}_x\text{Cu}_3\text{Ti}_4\text{O}_{12}$ ($0 \leq x \leq 0.2$), *Chem. Mater.* 22 (2010) 6–8.
- [23] B. Shri Prakash, A.K.B.R. Varma, Microstructural and dielectric properties of donor doped (La^{3+}) $\text{CaCu}_3\text{Ti}_4\text{O}_{12}$ ceramics, *J. Mater. Sci.: Mater. Electron.* 17 (2006) 899–907.
- [24] T.B. Adams, D.C. Sinclair, A.R. West, Giant barrier layer capacitance effects in $\text{CaCu}_3\text{Ti}_4\text{O}_{12}$ ceramics, *Adv. Mater.* 14 (2002) 1321–1323.
- [25] D.-K. Yoo, S.I. Yoo, Microstructures and dielectric properties of $\text{CaCu}_3\text{Ti}_4\text{O}_{12}$ polycrystalline ceramics, *Solid State Phenomena* 124–126 (2007) 143–146.
- [26] V. Dimitrov, T. Komatsu, An interpretation of optical properties of oxide and oxide glasses in terms of the electronic ion polarizability and average single bond strength, *J. Univ. Chem. Tech. Metall.* 45 (2010) 219–250.
- [27] T.B. Adams, D.C. Sinclair, A.R. West, Characterization of grain boundary impedances in fine- and coarse-grained $\text{CaCu}_3\text{Ti}_4\text{O}_{12}$ ceramics, *Phys. Rev. B* 73 (2006) 094124–94131.
- [28] D. Capsoni, M. Bini, V. Massarotti, G. Chiodelli, M. Mozzatic, C. Azzoni, Role of doping and CuO segregation in improving the giant permittivity of $\text{CaCu}_3\text{Ti}_4\text{O}_{12}$, *J. Solid State Chem.* 177 (2004) 4494–4500.